Spatially Confined FeF_3 Cathodes in N-Doped Carbon Nanotubes for Lithium Storage

Jun Li[a,b], Xifei Li[a,b,c] *, Mengyao Li[a,b], Qinting Jiang[a,b], Junqian Liu[a,b], Ruixian Duan[a,b], Guiqiang Cao[a,b], Jingjing Wang[a,b], Wenbin Li[a,b]

[a] *Shaanxi International Joint Research Center of Surface Technology for Energy Storage Materials, Institute of Advanced Electrochemical Energy and School of Materials Science and Engineering, Xi'an University of Technology, Xi'an, China*

[b] *Engineering Research Center of Conducting Materials and Composite Technology, Ministry of Education, Xi'an 710048, China, Key Laboratory of Advanced Batteries Materials for Electric Vehicles of China Petroleum and Chemical Industry Federation, Xi'an University of Technology*

[c] *Guangdong Yuanneng Technologies Co Ltd, Foshan, Guangdong, 528223, China*

E-mail address: xfli2011@hotmail.com

Experimental Section:

Preparation of FeF_3@N-CNTs

Typically, 1 g of dicyandiamide (DCDA) was dissolved in 30 mL of deionized water, stirred for 15 min, and then 200 mg ferric chloride ($FeCl_3$) was added into the above aqueous solution and stirred for 2 h to obtain a homogenous solution. The water was evaporated by heating the mixture at 80 °C under stirring in a water bath to produce the DCDA-Fe composite cluster. In the second step, the powder was heated under an Ar atmosphere at 800 °C for 2 h with a heating rate of 5 °C min^{-1} to obtained Fe_3C@N-CNTs. the FeF_3@N-CNTs was produced by fluorination of Fe_3C@N-CNTs at 300 °C for 2 h under Ar/NF_3 mixture gas (Ar/NF_3 volume ratio of 9:1). After cooling naturally, the final product of FeF_3@N-CNTs was immediately transferred into a glovebox to avoid air exposure.

Material Characterizations

The crystal and morphology structure were analyzed using X-ray diffraction (XRD, Rikagu SmartLab) with Cu Kα radiation, scanning electron microscopy (SEM, ZEISS, MERLIN Compact) and transmission electron microscopy (TEM, JEOL JEM-2100Plus) equipped with an energy-dispersive X-ray spectroscopy (EDS). The FeF_3 content was measured by thermogravimetric analysis (TGA, SDT Q600) in air flow under a heating rate of 10 °C·min^{-1}. The surface chemical states were analyzed by X-ray photoelectron spectroscopy (XPS, Thermo Fisher Scientific K-Alpha). The specific surface area and pore size distribution of the sample were studied using an Brunauer-Emmett-Teller method (BET, ASAP 2460). Raman spectra (Thermal Scientific DXR) were measured with a 532 nm laser.

Electrochemical Measurements

The FeF_3@N-CNTs and bare FeF_3 cathodes were prepared by mixing composites materials, acetylene black, and polyvinylidene fluoride with a weight ratio of 70:15:15 in a certain amount of N-methyl-2-pyrrolidone (NMP), The slurry was coated uniformly on Al foil and vacuum dried at 120 °C for 12 h. Using Celgard 2400 as separator and lithium foil as the counter electrode, the CR2023-type coin cells was

assembled for half-cell testing to evaluate the electrochemical performance. The electrolyte was 1.0 M LiFSI dissolved in a mixture of 1,2-dimethoxyethane (DME) and 1,1,2,2-tetrafluoroethyl-2,2,3,3-tetrafluoropropyl ether (TTE). The average areal mass loading of the FeF_3@N-CNTs on Al foil was approximately 0.9-1.0 mg cm^{-2}. The cell assembly was conducted in an argon-filled glove box (Vigor). The electrochemical performance was tested in the voltage of 1.0-4.0 V on Neware system, The cyclic voltammograms (CV) was measured on CHI660D and electrochemical impedance spectroscopy (EIS) was performed on an electrochemical workstation (PARSTAT MC) from 100 kHz to 0.1 Hz with an amplitude of 5.0 mV.

To estimate the electrochemical kinetics of the materials, the capacitive contribution can be fitted quantitatively using the following equation:

$$i(\mathrm{V}) = \mathrm{k}_1 v + \mathrm{k}_2 v^{1/2}$$

where i(V) is the peak current at the potential position of V, v represents the corresponding scan rate, and $\mathrm{k}_1 v$ and $\mathrm{k}_2 v^{1/2}$ are the current responses corresponding to capacitive contribution and diffusion controlled processes, respectively.

The Li^+ diffusion coefficient (D_{Li^+}) was calculated using GITT technique to expound the electrochemical reaction kinetics. The tested electrodes were activated at 0.3 A g^{-1} before the GITT tests. The D_{Li^+} value was calculated from the following equation:

$$D_{Li+} = \frac{4}{\pi\tau}\left(\frac{m_B V_m}{M_B A}\right)^2\left(\frac{\Delta E_s}{\Delta E_\tau}\right)^2$$

where m_B, M_B, and V_m are the mass, molecular weight and molar volume of active material, respectively. L and S are the thickness and area of the cathode, ΔE_S is the difference between open-circuit voltages after two adjacent relaxation processes, and ΔE_τ is the voltage difference between the beginning and termination during one titration step.

Scalability and commercial applications of synthetic methods

The synthesis strategy for FeF_3@N-CNTs can be extended to various transition metal-based composite materials, including Ni-based and Co-based systems. In addition, the gas-solid fluorination technique demonstrates remarkable versatility

beyond the synthesis of Ni-based and Co-based fluorides, it can be effectively applied to fluorinate carbides, nitrides, hydrides, oxides, and pure metal nanoparticles. These results demonstrate that the gas-solid fluorination technique possesses significant flexibility and scalability for future applications. We are currently conducting continuous optimization of both the composite material synthesis and gas-solid fluorination techniques. The development of these technologies will provide essential process engineering support for the potential commercial-scale production of high-energy-density fluoride-based cathode materials.

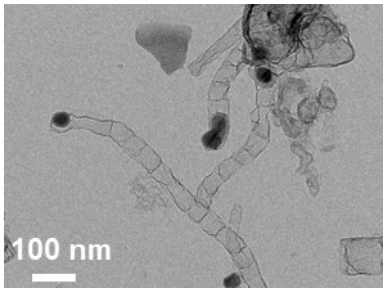

Fig. S1 The SEM image of Fe_3C@N-CNTs.

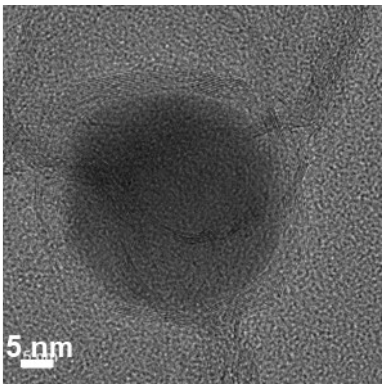

Fig. S2 The HRTEM image of Fe_3C@N-CNTs.

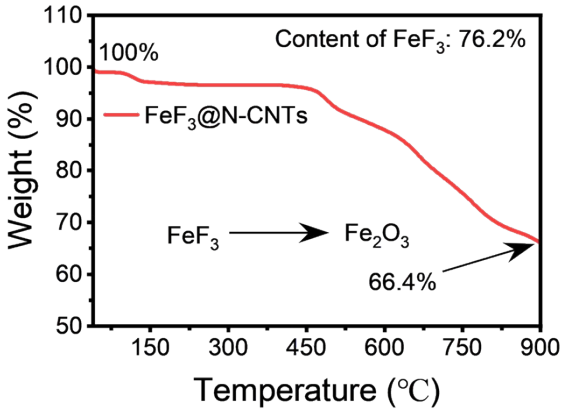

Fig. S3 TGA result of FeF_3@N-CNTs

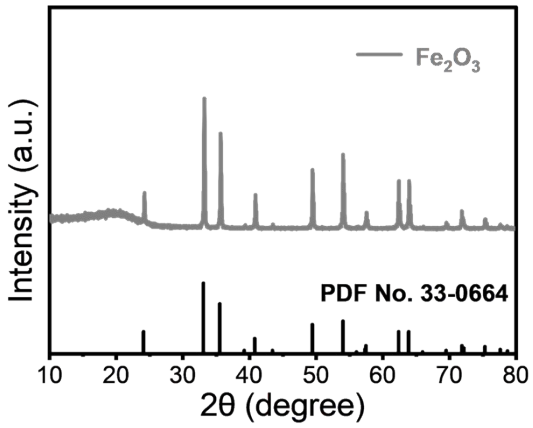

Fig. S4 XRD pattern of thermogravimetric analysis in air (from FeF_3@N-CNTs to Fe_2O_3)

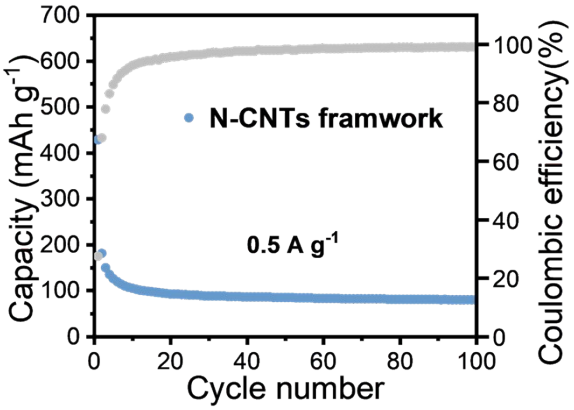

Fig. S5 Cycling performance of N-CNTs framework at 0.5 A g^{-1} after 100 cycles.

To determine the electrochemical capacity contribution of N-CNTs in the FeF_3@N-CNTs composite, the FeF_3@N-CNT composite material is treated with dilute

hydrochloric acid to obtain the N-CNT sample. At a current density of 0.5 A g^{-1}, the N-CNT sample without FeF_3 nanoparticles delivered a specific discharge capacity of only 78.6 mAh g^{-1} after 100 cycles, indicating that the high capacity of the composite material mainly depends on the electrochemical reactions of FeF_3 cathode.

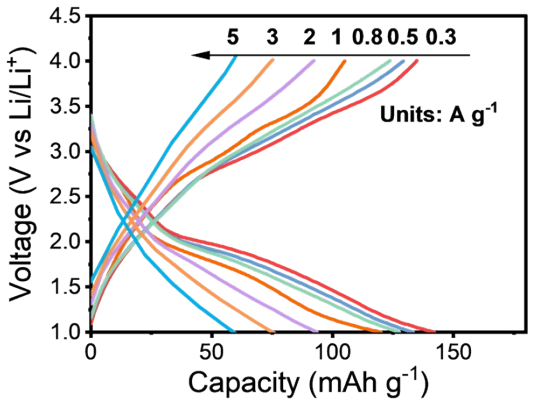

Fig. S6 Corresponding charge-discharge profiles of bare FeF_3.

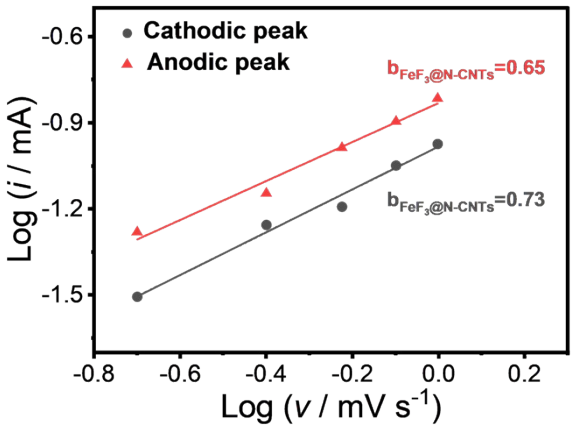

Fig. S7 Linear relationship of peak currents Log (*i*) versus scan rate Log (*v*) of the FeF_3@N-CNTs.

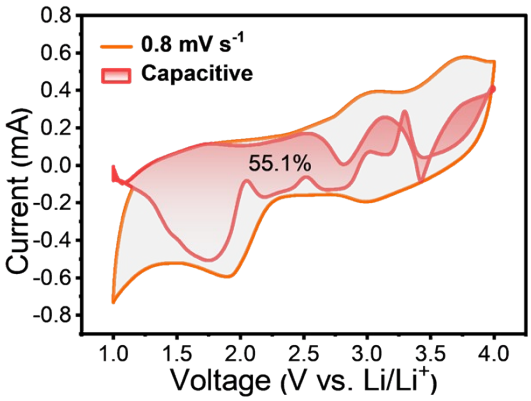

Fig. S8 CV curve of FeF_3@N-CNTs at 0.8 mV s^{-1} (shadow area showing the capacitive contribution).

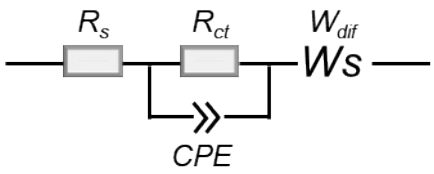

Fig. S9 The equivalent circuits of corresponding Nyquist plots.

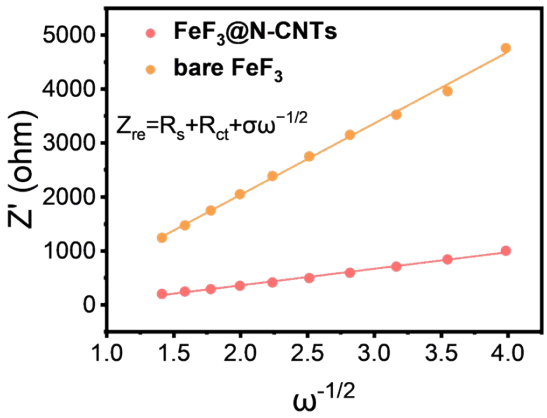

Fig. S10 Corresponding Nyquist plots of real parts of the complex impedance versus $\omega^{-1/2}$.

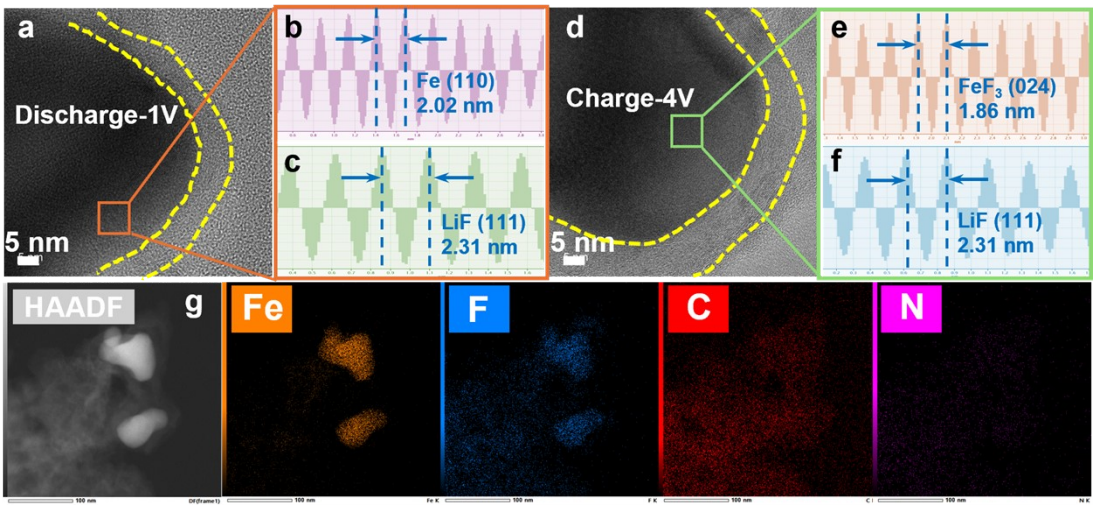

Fig. S11 (a, d) HRTEM image and corresponding (b-c, e-f) FFT pattern, (g) Elemental mapping images of FeF_3@N-CNTs cathode at different states after 40 cycles.

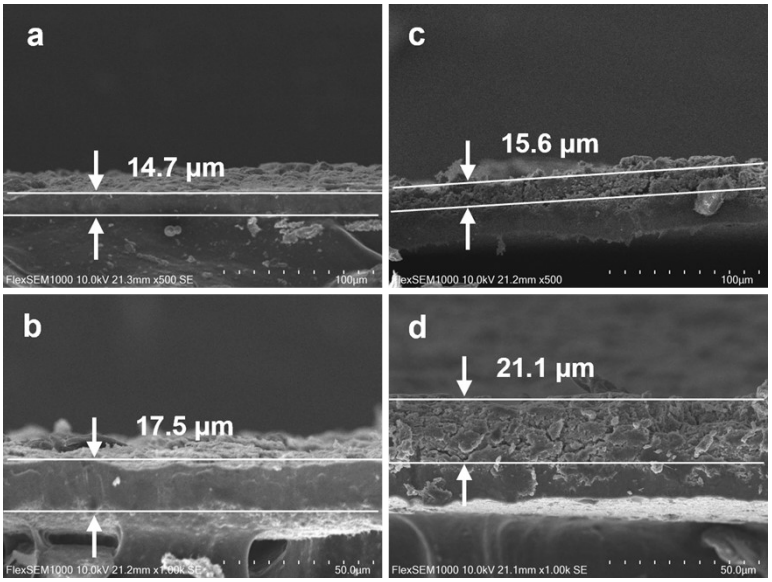

Fig. S12 Cross-sectional SEM images of (a-b) FeF_3@N-CNTs, (c-d) bare FeF_3 electrodes before and after lithiation.

Due to significant volume expansion of FeF_3 particles during lithiation, the electrode structure is susceptible to degradation, which becomes more severe with continued lithiation/delithiation cycles. The specific volume changes can be quantitatively assessed through cross-sectional SEM observations during the lithiated state. From the cross-sectional SEM image in Fig. S12, the thickness of the FeF_3@N-CNTs electrode increases from 14.7 μm to 17.5 μm after 100 cycles, which corresponds

to a 15.9 % increase in thickness (Fig. S12 a-b). As for the FeF_3 electrode, the thickness of the electrode increased from 15.6 μm to 21.1 μm, the thickness increased by 26.1 % (Fig. S12 c-d).

Table S1 The comparison of battery performance of FeF_3 based materials

Samples	Voltage range	Current density (mA g^{-1})	Specific capacity (mAh g^{-1})	Cycle number	Ref.
FeF_3·0.33H_2O@C	2-4.2V	237	172.2	200	*J. Power Sources,* **2022**, 547, 232014.
FeF_3/C	2-4.5V	20	126.3	100	*Electrochim. Acta,* **2018**, 281, 88.
FeF_3·0.33H_2O@HCN	2-4.5V	23	162	1000	*Carbon,* **2024**, 226, 119188.
Co doped FeOF@ACS	1.2-4V	1000	136	500	*J. Power Sources, **2024**, 604: 234510.*
Ni/Co dual-doped FeF_3·0.33H_2O	1.5-4.5V	1000	177	400	*Chem. Eng. J., **2023**, 451, 138774.*
FeF_3@C	1.5-4V	1000	210	400	*Rare Metals, **2023**, 42, 954.*
FeF_3·0.33H_2O@$AlPO_4$	1.2-4V	23	220	80	*J. Energy Storage, **2018**, 18, 103.*
FeF_3/C/LiF	1.5-4.5V	40	240	50	*J.Electroanal. Chem., **2018**, 810, 41.*
FeF_3@N-CNTs	**1-4 V**	**2000**	**110.6**	**5000**	**This work**

Table S2 The corresponding R_s and R_{ct} fitted values

	FeF_3@N-CNTs	bare FeF_3
R_s (Ω)	13.86	13.47
R_{ct} (Ω)	60.47	97.35